Applied Energy 373 (2024) 123860

Contents lists available at ScienceDirect

Applied Energy

journal homepage: www.elsevier.com/locate/apenergy

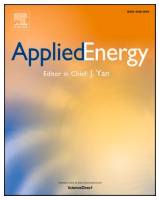

Decentralized intelligent multi-party competitive aggregation framework for electricity prosumers

Xiaoyuan Cheng [a,1], Ruiqiu Yao [a,1], Andrey Postnikov [b], Yukun Hu [a,*], Liz Varga [a]

[a] Department of Civil, Environmental & Geomatic Engineering, University College London, London WC1E 6BT, UK
[b] School of Engineering, University of Lincoln, Brayford Pool, Lincoln LN6 7TS, UK

HIGHLIGHTS

- A dynamic market competition model for prosumer aggregation.
- The solution state for the market to reach equilibrium is unique.
- A graph-based algorithm for the market model with edge computing.
- A proposed algorithm with a linear convergence rate.

ARTICLE INFO

Keywords:
Intelligent aggregation
Prosumers
Energy transition
Edge computing
Distributed energy resources
Graph-based consensus algorithm

ABSTRACT

Electricity management systems are experiencing significant challenges due to the increased penetration of distributed energy resources. Electricity flows in distribution networks are transforming from unidirectional to bi-directional form. Consumers are transitioning to prosumers with different characteristics, where they take more active roles in electricity generation and consumption. Aggregators are vital financial intermediary agents in the power system transitions, as they could aggregate energy profiles of prosumers. The market competition between aggregators and interactions between prosumers and aggregators are complex and dynamic, which requires a holistic framework to model the market competition. This paper proposes an intelligent aggregation framework with edge computing, enabling decentralized competition for multiple aggregators and prosumers, which can be solved with a graph-based consensus algorithm. This study mathematically proves the proposed algorithm's convergence guarantee and convergence rate. In addition, the proposed framework is applied to an open-source dataset to demonstrate its applicability. Lastly, a benchmark analysis is conducted to show that the proposed algorithm has better communication complexity than the benchmark algorithms.

1. Introduction

Electricity services are undergoing fundamental transitions on two fronts: penetration of distributed energy resources (DER) and decentralized decision-making with the Internet of Things (IoT). As shown in Fig. 1, the increasing penetration of DER units on low and medium-voltage networks transformed how electricity is generated, transmitted, and consumed [1]. Users in the power system are divided into two types, consumer and prosumer. Users without DER units are regarded as consumers as they can only purchase electricity from the electricity retailers and consume it. The electricity company in Fig. 1 includes distribution system operators, service providers, and retailers [2]. On the contrary, users with DER units are regarded as prosumers because they can produce electricity for self-consumption or export.

Major forms of DER include solar photovoltaics (PV), wind turbines, as well as electric vehicles (EVs) when vehicle-to-grid technologies are considered [3,4]. Such DER technologies enable users to produce electricity for self-consumption and sell the excess electricity to peers or upstream electric companies, i.e., becoming so-called prosumers. As a result, the electricity flow is no longer unidirectional but bidirectional.

Apart from the rise in DER penetration, the growing popularity of IoT technologies enables entities in the power system to communicate with each other through bidirectional information flow [5]. For example, prosumers not only can communicate with electric companies, but also communicate with peers via the Internet. More importantly, IoT

* Corresponding author.
E-mail address: yukun.hu@ucl.ac.uk (Y. Hu).
[1] Authors have equal contributions.

https://doi.org/10.1016/j.apenergy.2024.123860
Received 28 February 2024; Received in revised form 22 June 2024; Accepted 2 July 2024

Nomenclature

Acronyms

DER	Distributed energy resources
IoT	Internet of Things
PV	Photovoltaics
EV	Electric vehicle
MLMFG	Multi-leader-multi-follower game
VPP	Virtual power plant

Constants

A	Constant in battery degradation model [−]
R	Gas constant [J/(mol*K)]
T	Environment temperature [K]
$\lambda_{i,j}^{pro,ask}$	*Aggregator*$_i$'s bidding price to *prosumer*$_j$ [£/kWh]
β	Activation energy coefficient [−]
γ	Fixed-cost coefficient [£/kWh]
z	Power law factor [−]

Variables

$x_{i,j}$	Volume of electricity that *prosumer*$_j$ decides to sell to *aggregator*$_i$ [kWh]
$\lambda_i^{DA,bid}$	*Aggregator*$_i$'s bidding price at the day-ahead market [£/kWh]
$\lambda_{i,j}^{pro,ask}$	*Aggregator*$_i$'s bidding price to *prosumer*$_j$ [£/kWh]
c	Number of battery cycles from the initial state of the battery
μ_x, μ_z	Langrangian multipliers for inequality constraints [−]

Functions

$F_i(x)$, $G_i(z)$	Indicator functions [−]
$L_0(x, z, \mu_x, \mu_z, \lambda)$	Lagrangian function [−]
$V^k(\bullet)$	Lyapunov function of the optimization problem [−]

Indices and sets

$\mathbb{I}$	N-dimensional identity vector
χ	Closed convex feasible sets of trading electricity matrix
$\mathbf{\Lambda}$	Closed convex feasible sets of asking price matrix
C_a, D_b	Convex feasibility sets
V	Set of nodes on a graph
$\mathscr{E}$	Set of the edges on a graph

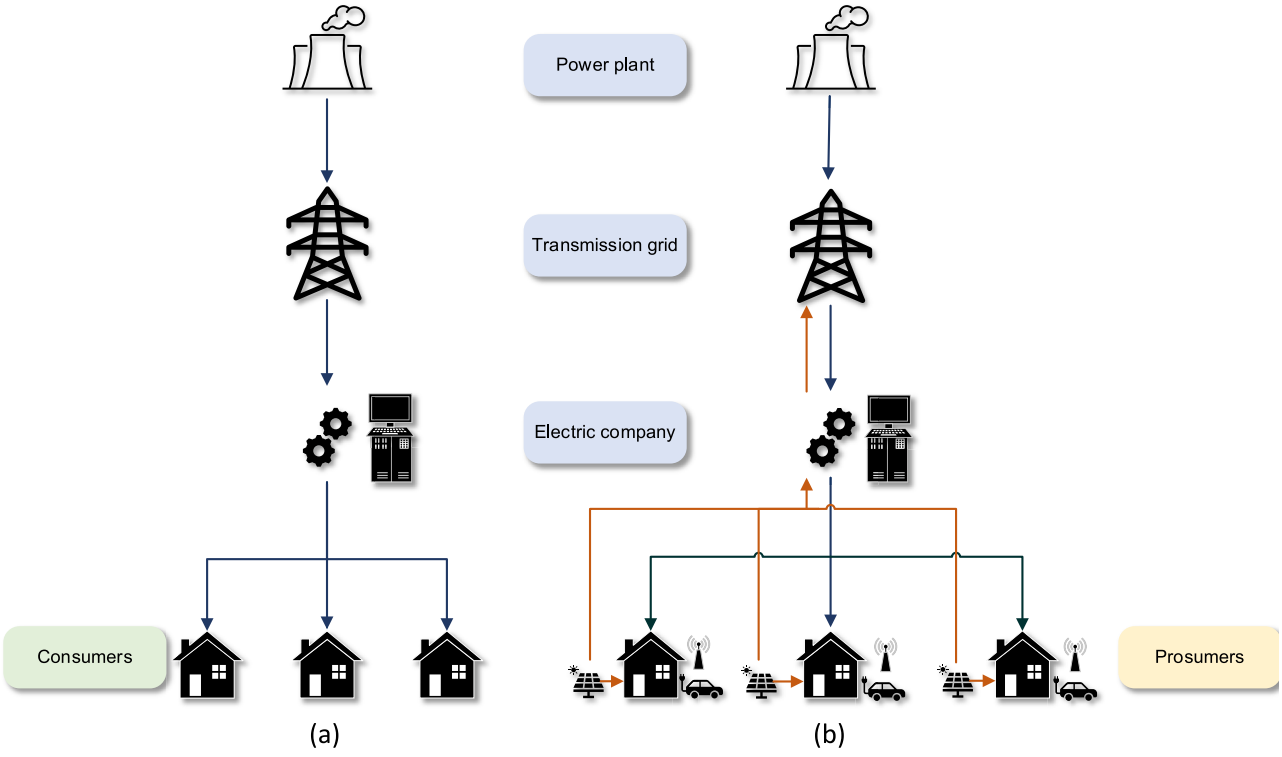

Fig. 1. Power system transitions. (a) schematic drawing of the unidirectional power flow with consumers under the current power system structure; (b) schematic drawing of bidirectional power flow with prosumers for future power system structure.

technologies provide computation resources to users, enabling local data processing and storage. The computational ability provided by IoT technologies makes edge computing [6] an emerging computation technique in the energy system. Edge computing can provide low-latency communication, which is crucial for decentralized decision-making [7].

The decentralization of electricity generation and decision-making spawned novel approaches for prosumers to participate in electricity markets. There are two pathways for prosumers to trade surplus electricity: 1) selling excess electricity to local consumers. 2) selling aggregated excess electricity to the upstream grid, which is connected with prosumers. The first trading pathway is called peer-to-peer (P2P) trading, and the second pathway is called virtual power plant (VPP). P2P sharing systems enable prosumers to negotiate electricity prices with peers within the community, then trade electricity and flexibility services through the negotiated contracts [8]. The negotiated price is also

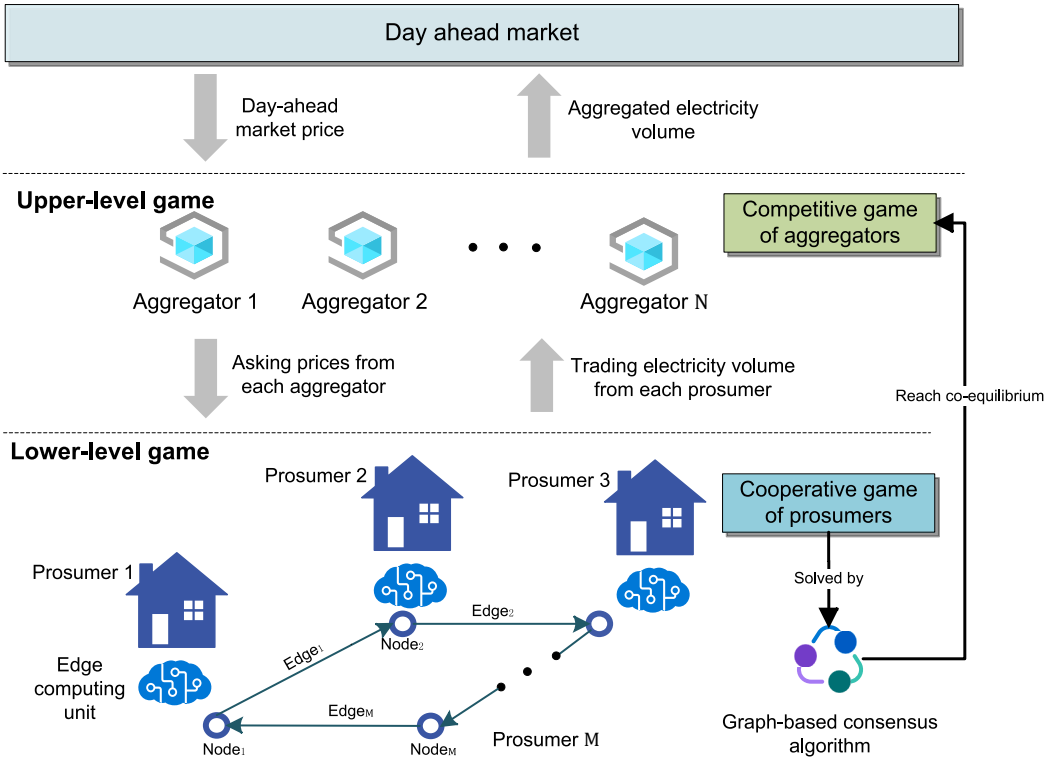

Fig. 2. Intelligent aggregation architecture.

named as domestic price, which is usually set lower than retail prices to encourage electricity sharing [2]. VPP is a framework to coordinate and export excess local electricity from prosumers beyond local communities to a list of regional electricity markets, including futures and forward markets, day-ahead markets, ancillary markets, intraday markets, and real-time balancing markets [9–14]. Such a framework allows VPPs to balance the electricity grids in multiple time scales, ranging from sub-hourly (real-time balancing market) to monthly or yearly (futures and forward market) [15]. VPP schemes are hierarchical aggregation management processes that coordinate clusters of DER units to profit from participating in the electricity market. VPP schemes can integrate EV load management, such as energy storage and controllable loads, into system coordination through Vehicle-to-Grid (V2G) services [15].

The maximization problem of VPP is formulated as an economic dispatch problem where the objective function is the total expected income in a given time period. In addition, the economic dispatch problems are subject to a list of constraints [16], such as energy balance constraints, production unit constraints (output limit and ramp limit), and transmission network constraints. To solve the constrained economic dispatch problem, the current VPP management scheme utilizes various optimization techniques, such as linear programming (LP) [17,18], mixed-integer linear programming (MILP) [19–21], nonlinear programming (NLP) [22,23], and mixed-integer nonlinear programming (MINLP) [24,25]. These studies in electricity aggregation are designed in centralized architectures, where DER owners need to grant aggregation operators access to their assets. Such a centralized decision-making architecture requires a central computing unit to collect operational statuses from DERs and provide operational instructions based on optimization results [20,22]. By comparison, a decentralized architecture enables DER owners not to share the operational access with the aggregator operators to preserve data privacy, e.g., system specifications and detailed operation status. The next section reviews the state-of-art literature on privacy-preserving aggregation.

1.1. Motivation

Aggregators are virtual intermediaries representing prosumers in the electricity service markets [26]. Obi, Slay, and Bass [27] provided a detailed review of the viable grid services aggregators can provide. The grid services include asset aggregation, dispatch standby generation, and ancillary services. The business models of aggregators are built on providing the above-mentioned services [28]. Iria et al. [29] proposed a privacy-preserving bidding strategy for an aggregator to bid in the day-ahead market. The bidding strategy is designed to ensure the security of the distribution network. The bidding strategy is obtained by applying the alternating direction method of multipliers (ADMM). Shomalzadh, Scherpen, and Camlibel [30] also research the optimal bidding of an aggregator in the day-ahead market with detailed proof of the convex bi-level problem. Apart from the research above, the game theory formulation has recently gained popularity in aggregation research, particularly the multi-leader-multi-follower game (MLMFG).

The MLMFG [31] models are well suited to formulate the dynamic market interaction in energy markets. MLMFG is a game theory model to compromise among multiple interacting decision units and competition among decision-makers of multiple hierarchical systems. A collection of players at the upper-level compete in a Nash game [32] constrained by the equilibrium conditions of another Nash game at the lower level. The players in the upper- and lower-levels are called leaders and followers, respectively. The optimal strategies of the leaders are determined based on the conjectured reactions of the followers. In 2020, Xiao et al. [33]

used the MLMFG model to propose a privacy-preserving aggregation framework to participate in the day-ahead market, where aggregated prosumers are the leaders and end-users are followers. The game model is formulated as MILP. In 2023, Hong et al. [34] adopted the MLMFG model to consider the optimal aggregation in both the day-ahead market and the local electricity market, and the diagonalisation algorithm solves the game model. Thus, the MLMFG is an applicable methodology to model the prosumer aggregation process.

1.2. Contributions

In terms of solving the electricity aggregation MLMFG model, edge computing emerges as a viable technological pathway to solve the model with the penetration of IoT technology because edge computing offers the ability to implement a fully decentralized optimization algorithm with low communication latency. A systematic framework is needed to implement the consensus algorithm with edge computing to solve the MLMFG model. However, to the best of the authors' knowledge, no similar research has been reported yet. Thus, the contribution of this study is summarized as follows:

- Proposed an intelligent aggregation framework, i.e., a multi-aggregator MLMFG model, which can be solved by a novel graph-based consensus algorithm. The multi-aggregator MLMFG model has been proven with the existence and uniqueness of the solution to the model. The novel graph-based consensus algorithm has been proven to converge with a linear convergence rate.
- Demonstrated the applicability of the proposed intelligent aggregation framework in a case study. The proposed algorithm is also compared with state-of-the-art algorithms using benchmark analysis. The proposed algorithm has less communication complexity than the state-of-the-art algorithms.

1.3. Paper organization

The rest of the paper is organized as follows: Section 2 explains the mathematical formulation of the intelligent aggregation framework. Section 3 provides the simulation results of the proposed framework and algorithm. Section 4 concludes the study and provides future research directions.

2. Intelligent aggregation framework

The proposed decentralized intelligent aggregation framework is shown in Fig. 2. In the proposed framework, a prosumer is regarded as a household with ownership of the DER units. Each prosumer is assumed to have the computational ability in a standalone decision-making module, such as edge computing embedded smart meters [35]. The prosumers and aggregators are able to send bidding and asking signals to each other through internet protocols. The Distribution System Operator (DSO) also broadcasts the network constraints to the aggregators as well as prosumers.

During market interactions, a prosumer cooperates with other prosumers to maximize the joint welfare of the prosumers. In the meantime, an aggregator competes with other aggregators to maximize the expected utility by changing to the asking price (also referred to as the offer price). Thus, such optimization problems are a bi-level optimization problem of a MLMFG. The MLMFG model can be subsequently solved by the proposed graph-based consensus algorithm. The optimized result implies the fact that both levels of the market reach equilibrium at the same time. Hence, the system reaches a co-equilibrium state. It should be noted that aggregators are responsible for two stages of actions, where aggregators first accumulate electricity from prosumers and then sell it to the wholesale market.

2.1. Bi-level market equilibrium model

The market interactions during the aggregation process can be divided into two games: an upper-level game, in which aggregators participate, and a lower-level game, in which prosumers participate. In the case of the aggregation process, the leaders are aggregators, while the followers are prosumers. Knowing the optimal strategy of the aggregators, prosumers compute the optimal strategy of their parameterized Nash game, which can differ from the aggregators' conjecture in case of multiplicity of the solutions of the prosumer' game.

2.1.1. MLMFG formulation

In the game theory formulation of MLMFG, the upper-level game among leaders can be expressed as [36]:

$$\begin{aligned} &\min_{e_i} \quad F_i(e_i, e_{-i}, y) \\ &\text{s.t.} e_i \in E_i \end{aligned} \tag{1}$$

All leaders $\forall i = 1, 2 \ldots, M$ aim to solve the optimization problem represented by optimization problem (1). $F_i(\bullet)$ is the utility function for $leader_i$, and E_i is the feasible set of $leader_i$'s strategy e_i. The optimal strategy e_i^* depends on the strategies of other leaders in the upper-level game, where the strategies of other leaders are denoted as $e_{-i} := [e_1, e_2, \ldots, e_{i-1}, e_{i+1}, \ldots, e_M]$.

The lower-level game among followers can be expressed as [36]:

$$\begin{aligned} &\min_{y_j} \quad \theta_j\left(y_j, y_{-j}, e\right) \\ &\text{s.t.} y_j \in Y_j(e) \end{aligned} \tag{2}$$

All followers $\forall j = 1, 2 \ldots, N$ aim to solve the optimization problem represented by optimization problem (2). $\theta_j(\bullet)$ is the utility function for $follower_j$. Y_j is the feasible set of $follower_j$'s strategy y_j. The optimal strategy of $follower_j$ depends on the strategies of other followers in the lower-level game. The strategies of other followers are denoted as $y_{-i} := \left[y_1, y_2, \ldots, y_{j-1}, y_{j+1}, \ldots, y_N\right]$. It should be noted that the followers' objective functions and feasible sets depend on the leaders' strategies vector e. The following Section 2.1.2 explains the formulation of the bi-level market co-equilibrium model based on MLMFG.

2.1.2. Bi-level market co-equilibrium model

This study proposes a unified bi-level market co-equilibrium model for decentralized intelligent multi-party aggregation with DER-enabled prosumers. The co-equilibrium model is proposed for a distribution network with M aggregators and N prosumers. The volume of electricity that $prosumer_j$ decides to sell to $aggregator_i$ is denoted as $x_{i,j}$. The volume of electricity $x_{i,j}$ can be expressed as a set $\{x_{i,j} | x \in \mathbb{R}, i = 1, 2, \ldots, M; j = 1, 2 \ldots, N\}$. This trading volume of electricity in the distribution network forms a real-valued matrix of $\boldsymbol{X} \in \mathbb{R}^{M \times N}$. The volume of electricity that $aggregator_i$ receives is denoted $x_{i,*} = \left[x_{i,1}, x_{i,2}, \ldots x_{i,N}\right]^T$, which is the i^{th} column vector of matrix $\boldsymbol{X}$. The volume of electricity that $prosumer_j$ decides to sell is denoted as $x_{*,j} = \left[x_{1,j}, x_{2,j}, \ldots x_{M,j}\right]$, which is the j^{th} row vector of $\boldsymbol{X}$.

The business model of aggregators is important because it reflects the motivations behind aggregators' desire to facilitate electricity aggregation. In the proposed market model, aggregators' revenue accrues when

they sell aggregated electricity in the day-ahead market at the current day-ahead price. It is also important to consider the cost of aggregation. This study assumes that the aggregators are the price-takers of the day-ahead market, which means aggregators' decisions do not affect the day-ahead market price. The aggregation cost should consider two components: variable cost and fixed cost [37]. As a result, the utility function of aggregators is formulated as Eq. (3):

$$\underset{\lambda_{i,j}^{pro},}{arg\,max} \sum_{j=1}^{N} \left(\lambda_i^{DA,bid} - \lambda_{i,j}^{pro,ask} - \gamma\right) x_{i,j}, i = 1, 2, \ldots M \tag{3}$$

$$s.t. \underline{\lambda}_{i,j}^{pro,ask} \le \lambda_{i,j}^{pro,ask} \le \overline{\lambda}_{i,j}^{pro,ask}, \tag{3.a}$$

where $\lambda_i^{DA,bid}$ is the aggregators' bidding price at the day-ahead market, making $\lambda_i^{DA,bid} x_{i,j}$ the revenue for aggregating $x_{i,j}$ amount of electricity. The decision variable $\lambda_{i,j}^{pro,ask}$ is the asking price of $aggregator_i$ promise to pay $prosumer_j$, which makes $\lambda_{i,j}^{pro,ask} x_{i,j}$ the variable cost of aggregators. The fixed cost component is parameterized by a fixed-cost coefficient γ. Apart from the utility function, the optimization problem of aggregators also includes the constraint (3.a). $\underline{\lambda}_{i,j}^{pro,ask}$ and $\overline{\lambda}_{i,j}^{pro,ask}$ are the lower and upper bound for the asking price at the prosumer-aggregator market to ensure the profitability of aggregators and prevent excess profits. The price bounds are pre-determined by the regulatory body to ensure the competitiveness of the market.

Eq. (4) indicates the utility function of the prosumer which consists of three terms. The first term $\lambda_{i,j}^{pro} x_{*,j}$ represents the payments received from aggregators, which is the revenue for prosumers. On the other hand, this study treats battery degradation as utility loss for prosumers to participate in aggregations. The battery degradation model is based on the power law model in [38].

$$\underset{x_{*,j}}{arg\,max} \sum_{i=1}^{M} \lambda_{i,j}^{pro} x_{*,j} - \mathbb{I}^T A e^{\left(\frac{\beta x_{*,j}}{RT}\right)} c^z + x_{*,j}^T \frac{\partial A e^{\left(\frac{\beta x_{*,j}}{RT}\right)} c^z}{\partial x_{i,j}}, j = 1, 2, \ldots N \tag{4}$$

$$s.t. x_{*,j} \le \overline{x}_{*,j} \tag{4.a}$$

$$\underline{x}_{i,*}^{DA} \le x_{i,*} \le \overline{x}_{i,*}^{network}, \tag{4.b}$$

where A is a constant. R and T are the gas constant and temperature, respectively. β is the activation energy coefficient. c is the number of battery cycles from the initial state of the battery. z is the power law factor. The third term is a first-order utility derivative term to ensure the convergence of the game. The optimization problem of prosumers also includes the constraint (4.a) and (4.b). Constraint (4.a) is the maximum battery discharge rate, and it indicates the upper bound of $x_{*,j}$. Constraint (4.a) can be treated as the row-wise constraint on the trading electricity matrix $\boldsymbol{X}$. In addition, the trading electricity matrix $\boldsymbol{X}$ is bounded column-wise by the $\underline{x}_{i,*}^{DA}$, the minimum bidding size at the DA market, and $\overline{x}_{i,*}^{network}$, the network constraint is informed by the distribution system operator. The proof of the market co-equilibrium model is explained in **Appendix A. Market Equilibrium Proof**.

2.2. Solving the bi-level model with a graph-based consensus algorithm

In this section, we propose a novel graph-based consensus algorithm to solve the intelligent aggregation problem with inequality constraints. Section 2.2.1 explains how the proposed algorithm considers inequality constraints. Section 2.2.2 describes how the proposed algorithm operates on a graph.

2.2.1. Considering inequality constraints

Since the standard version of ADMM is only suitable for decomposable convex problems with equality constraints, in order to deal with optimization problems with inequality constraints, the ADMM algorithm is modified so that it can solve distributed optimization problems with both equality and inequality constraints.

$$\begin{aligned} &minf(x) + g(z) \\ &\text{s.t.} Ax + Bz = c \\ &F_i(x) \le 0\ i = 1, 2, \ldots, p \\ &G_i(z) \le 0\ i = 1, 2, \ldots, q \end{aligned} \tag{5}$$

Modified optimization problem (5) has variables $x \in \mathbb{R}^n$ and $z \in \mathbb{R}^m$, where $A \in \mathbb{R}^{p \times n}$, $x \in \mathbb{R}^{p \times m}$, and $c \in \mathbb{R}^p$. Note that there are countable convex inequalities that constrain the feasible set of decision vectors x and z. The $F_i(x)$ and $G_i(z)$ are extended-value indicator functions, which are equivalent to:

$$F_i'(x) = \begin{cases} 0, & F_i \le 0 \\ \infty, & F_i > 0 \end{cases}, i = 1, 2, \ldots, p \tag{6}$$

$$G_i'(z) = \begin{cases} 0, & G_i \le 0 \\ \infty, & G_i > 0 \end{cases}, i = 1, 2, \ldots, q \tag{7}$$

where $F_i' : \mathbb{R}^n \to \mathbb{R} \cup \infty$ and $G_i' : \mathbb{R}^n \to \mathbb{R} \cup \infty$ are closed, proper and convex. The Lagrangian function of the reconstructed form is:

$$\begin{aligned} L_0(x, z, \mu_x, \mu_z, \lambda) = f(x) + g(z) + \rho \Big/ 2 \Big(&\left\| F_1'(x) \right\|^2 + \left\| F_2'(x) \right\|^2 + \ldots \\ &+ \left\| F_p'(x) \right\|^2 \Big) + \langle \mu_x F'(x) \rangle + \rho \Big/ 2 \Big(\left\| G_1'(z) \right\|^2 \\ &+ \left\| G_2'(z) \right\|^2 + \ldots + \left\| G_q'(z) \right\|^2 \Big) + \langle \mu_z G'(z) \rangle \\ &+ \rho \Big/ 2 \Big(\|Ax + Bz - c\|^2 + \langle \lambda Ax + Bz - c \rangle \Big) \end{aligned} \tag{8}$$

For Eq. (8), $F'(\bullet) = \left[F_1'(\bullet), F_2'(\bullet), \ldots, F_p'(\bullet)\right]$ and $G'(\bullet) = \left[G_1'(\bullet), G_2'(\bullet), \ldots, G_q'(\bullet)\right]$ are the gradient of extended-value indicator functions $F_i(x)$ and $G_i(z)$. $\mu_x = \left[\mu_1^x, \mu_2^x, \ldots, \mu_p^x\right]$ and $\mu_z = \left[\mu_1^y, \mu_2^y, \ldots, \mu_q^y\right]$ are Langrangian multipliers for inequality constraints. λ is the Langrangian multiplier for equality constraint. Then, the iterative body of ADMM is shown as below:

$$x^{k+1} = argmin\left(x, z^k, \mu_x^k, \mu_z^k, \lambda^k\right) \tag{9.a}$$

$$z^{k+1} = argmin\left(x^{k+1}, z, \mu_x^k, \mu_z^k, \lambda^k\right) \tag{9.b}$$

$$\mu_x^{k+1} = \mu_x^k + \rho F'\left(x^{k+1}\right) \tag{9.c}$$

$$\mu_z^{k+1} = \mu_z^k + \rho G'\left(z^{k+1}\right) \tag{9.d}$$

$$\lambda^{k+1} = \lambda^k + \rho(Ax + Bz - c) \tag{9.e}$$

However, there is a problem with the gradient of indicator functions of $\left\| F_i'(x) \right\|^2$ and $\left\| G_i'(z) \right\|^2$. Due to the property of a normal cone, it is not possible to get sets of subdifferentials of the group of indicator functions. The extend-value indicator functions can be approximated to obtain gradients:

$$F_i'(x) = max(0, F_i(x)^m), i = 1, 2, \ldots, p \tag{10}$$

$$G_i'(x) = max(0, G_i(x)^m), i = 1, 2, \ldots, q \tag{11}$$

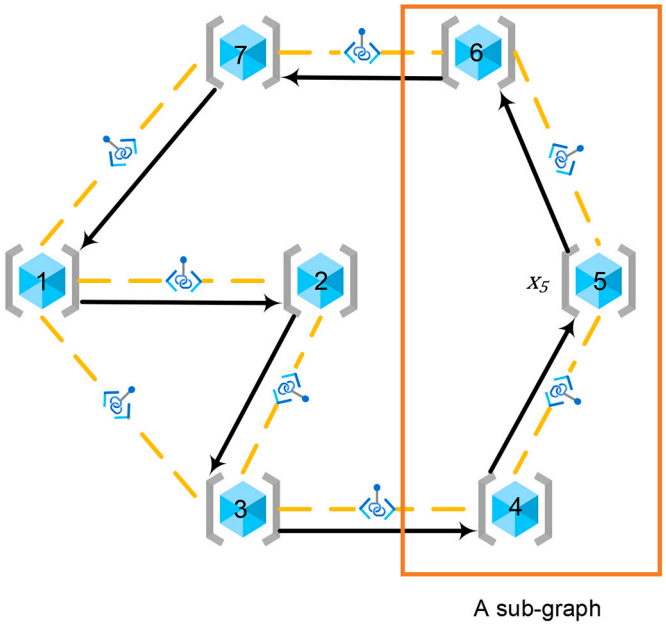

Fig. 3. Schematic diagram of the graph-based consensus algorithm.

Then the difference of the function is solvable, the desired solution of the ADMM functions can be solved in the following sub sections.

2.2.2. Convergence analysis

On the analysis that ADMM can be equivalent to the Lyapunov function in analytical optimization [39] with a similar approach as [40]:

$$V^k = \frac{1}{\rho}\|\mu_x^* - \mu_x^k\|^2 + \frac{1}{\rho}\|\mu_z^* - \mu_z^k\|^2 + \frac{1}{\rho}\|\lambda^* - \lambda^k\|^2 + \rho\|Bz^{k+1} - Bz\|^2, \quad (12)$$

where k is the iteration time. When $k\to\infty$, the parameter $(\mu_x^k, \mu_z^k, \lambda^k,)$ shows an incrementally stable behavior.

Theorem 1. *The duality theory claims that the relationship between primal solution the solution of dual problems*:

$$L_0(x, z, \mu_x^*, \mu_z^*, \lambda^*) \geq L_0(x^*, z^*, \mu_x^*, \mu_z^*, \lambda^*) \quad (13)$$

where L_0 is the Lagrangian function and x^*, z^* is the solution of primal.

Theorem 2. The Theorem 2 states primal feasibility and convergence of the primal objective function value:

$$\lim_{k\to\infty} r_g^k = 0, \quad (14.a)$$

$$\lim_{k\to\infty} r_h^k = 0, \quad (14.b)$$

$$\lim_{k\to\infty} f^k = f^*, \quad (14.c)$$

$$\lim_{k\to\infty} g^k = g^*, \quad (14.d)$$

where $r_g := F_i'(x)$ and $r_h := Ax + Bz - c$. The convergence of ADMM needs to be identified when inequality constraints are involved, the proof can be obtained through some lemmas. The proof is sketched as below, while similar lemmas without inequality constrains can be found in the appendix of [39].

Lemma 1. *The dual variables* μ_x^k, μ_z^k are non-negative for all iterations, i. e., it holds that $\mu_x^k \geq 0$ and $\mu_z^k \geq 0$ for all $k \in \mathbb{N}$.

Lemma 2. *The difference between the optimal objective function value and its value at the* $(k+1)^{th}$*iterate can be bounded as*:

$$f(x^*) + g(z^*) - f(x^{k+1}) + g(z^{k+1}) \leq \left\langle \mu_x^*, r_g^k \right\rangle + \left\langle \lambda^*, Ax^{k+1} + Bz^{k+1} - c \right\rangle \quad (15)$$

Lemma 3. The difference between the value of the objective function at the $(k+1)^{th}$ iterate and its optimal value can be bounded by linear form of μ, λ, ρ.

Lemma 4. *The absolute convergence of Lyapunov function* Eq. (12):

$$\left\{ \sum_{k=0}^{\infty} \left(\|\mu_x^* - \mu_x^k\|^w + \|\mu_z^* - \mu_x^k\|^2 + \|\lambda^* - \lambda^k\|^2 + \rho\|Bz^{k+1} - Bz\|^2 \right) \right\} \leq \sum_{k=0}^{\infty} (V^k - V^{k+1}) \leq V^0 \quad (16)$$

The hold of Lemma 4 can be obtained from the first three lemmas. The convergence of value ensures the convergence of ADMM with inequalities.

2.2.3. The graph-based ADMM consensus algorithm

The communication networks can be understood as an undirected graph $g(V, \mathscr{E})$, where $V = \{1, 2, \ldots, P\}$ is the set of nodes and $\mathscr{E} \in V \times V$ is the set of edges. The cardinality of this set is represented by P and E. An edge is defined as $(i, j) \in \mathscr{E}$, indicating that nodes i and j can share information. The cardinality of P is denoted as $|P|$. To construct the desired graph, each prosumer is assumed only to be connected with their neighboring prosumers within a certain distance because long-distance communication can be energy-consuming. The system optimization efficiency can be improved by following a *Hamiltonian path*, which is a path that visits each vertex exactly once [41]. The existence of a Hamiltonian path in a graph can be checked with a polynomial time, which is also known as the Non-deterministic Polynomial complete problem [42]. In a prosumer-aggregator network, the graph-based consensus algorithm searches this path on the constructed graph, and the shortest Hamiltonian is employed to update the agents' utility functions to minimize energy consumption.

Once finding the shortest Hamiltonian path in the path, each node with its neighbors can be constructed as a subgraph, and then there will be $|P|$ subgraphs in the system. Two adjacent nodes in a subgraph can share information. When prosumers are equipped with edge computing units, the solution of the matrix $\boldsymbol{X}$ can be stored locally. Previous researchers [43,44] have proved that the optimization in a subgraph can reach a global equilibrium. In the optimization process, a node with updated information will share information with its neighbors, and then using the graph-based ADMM algorithm can completely decentralize the process. The starting point of the traversal can be any node in the Hamiltonian path. The co-equilibria point of the lower-level game in the graph-based method [44–46] can be defined as follows:

$$\begin{aligned} &\min_{x_{i,*}} \sum_{p\in[n]} f_j\left(x^p_{*,j}, x^p_{*,-j}\right), \\ &\text{s.t.} \mathbb{I} \otimes \mathrm{X} = \mathrm{Y}, \\ &\text{s.t.} \left[\mathrm{x}^{\mathrm{j}}_{*,\mathrm{j}}, \mathrm{x}^{\mathrm{j}}_{*,-\mathrm{j}}\right] = \mathrm{Y}_{\mathrm{j}}, \end{aligned} \tag{17}$$

where $\otimes$ is the Kronecker product. $\mathbb{I}$ indicated the connection of subgraphs. In each iteration of the lower-level game, the optimization step $x^{(p+1)}_{*,j} = \underset{x_{*,j}}{arg\,min}\ L_0\left(x_{*,j}, \mu^{(p)}_x, \mu^{(p)}_z, \lambda^{(p)}\right)$ is conducted, and updated results will be shared with the connected nodes. After each cyclic iteration in the Hamiltonian path, the matrix X will be delivered to the aggregators. The aggregator will compete to maximize its own utility in Eq. (3). The optimization iteration will continue until the game achieves an equilibrium point. The details of the graph-based ADMM algorithm are demonstrated with the pseudocode shown in Algorithm 1.

Algorithm 1. Graph-based consensus ADMM.

Input: the amount of electricity of each prosumer $i = 1, \ldots M$
Output: the matrix $\boldsymbol{X}$, and the prices λ^{pro} offered by each aggregator
Initialize: the randomized first-order utility derivative term, $i = 1, \ldots M, j = 1, \ldots, N; p \leftarrow 0$
While $\sum_i d(G_i(x^{p+1}_{i,*}) - G_i(x^p_{i,*})) < \epsilon$:
{Update the lower-level game}
For j from 1 to N:
L1. Search the followers' game solution by graph-based consensus ADMM, updating the primal and dual variables for the augmented Lagrange function in $\sum_i d(G_i(x^{p+1}_{i,*}) - G_i(x^p_{i,*}))$
L2. Sharing with the local graph by connection matrix in the Hamiltonian path
L3. Update the incentive rewards
$p \leftarrow p + 1$
{Update the upper-level game}
For i from 1 to M:
U1. Update the transaction prices $\lambda^{pro}_{i,*}$ for each aggregator
End

volume information through the private communication link (yellow dash line). For example, node 5, with neighboring node 4 and node 6, constructs a subgraph. Fig. 4 shows prosumers sequentially updating the $x_{*,j}$ along the Hamiltonian path (from left to right) with the progression of iteration steps (from top to bottom).

2.2.4. Convergence rate analysis

This section proves that the convergence rate of the proposed algorithm is linear.

Proof.

When step k is sufficiently large:

$$\begin{aligned} &\frac{\partial \mu^{\mathrm{k}}_{\mathrm{x,j}}\left(\mathbb{I}_{\mathrm{D_b}}\left(\mathbf{x}^{\mathrm{k}}_{*,\mathrm{j}}\right)\right)}{\partial \mathrm{x}_{\mathrm{i,j}}} + \frac{\partial \frac{\rho}{2}\left|\left|\mathbb{I}_{\mathrm{D_b}}\left(\mathbf{x}^{\mathrm{k}}_{*,\mathrm{j}}\right)\right|\right|}{\partial \mathrm{x}_{\mathrm{i,j}}} + \frac{\partial \mu^{\mathrm{k+1}}_{\mathrm{z,i}}\left(\mathbb{I}_{\mathrm{C_a}}\left(\mathbf{x}^{\mathrm{k}}_{\mathrm{i},*}\right)\right)}{\partial \mathrm{x}_{\mathrm{i,j}}} = 0 \\ &\mathbb{I}_{\mathrm{C_a}}\left(\mathbf{x}^{\mathrm{k}}_{\mathrm{i},*}\right), \mathrm{a} = 1, 2, \ldots \mathrm{A} \\ &\mathbb{I}_{D_b}\left(\mathbf{x}^{k}_{*,j}\right), b = 1, 2, \ldots \end{aligned} \tag{18}$$

Fig. 3 shows a schematic drawing of the proposed graph-based consensus algorithm. Once the Hamiltonian path is constructed, a node with two adjacent nodes can form a sub-graph to share the trading

Eq. (18) indicates the constraints for both levels can be satisfied when the step k is sufficiently large. By applying convexity of $-f\left(\boldsymbol{x}^*_{i,j}\right)$ and Eq. (A.16), it can be obtained that:

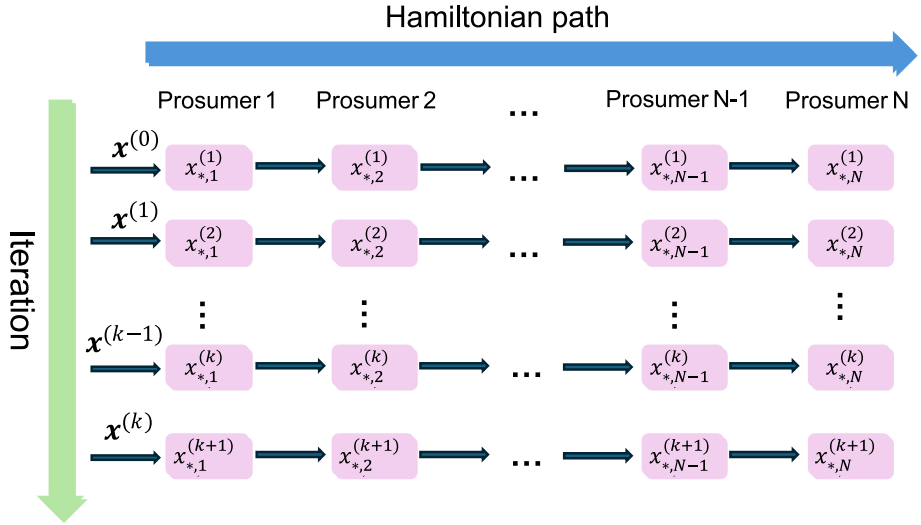

Fig. 4. Iteration details of the proposed algorithm.

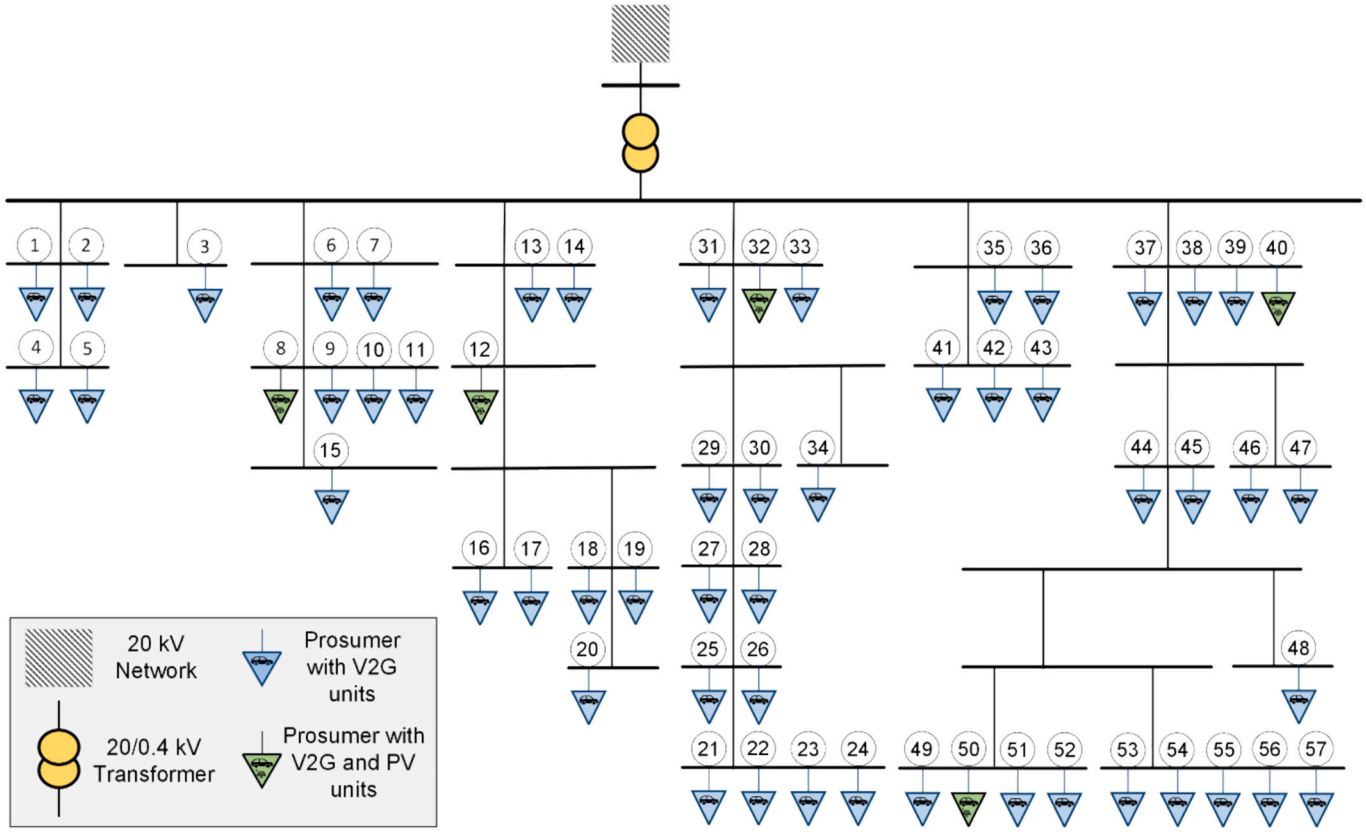

Fig. 5. LV electric distribution network.

Table 1
The day-ahead prices used in the case study.

Time	1	2	3	4	5	6	7	8	9	10	11	12
Price (£/kWh)	0.070	0.064	0.067	0.070	0.065	0.060	0.084	0.100	0.103	0.080	0.074	0.072

Time	13	14	15	16	17	18	19	20	21	22	23	24
Price (£/kWh)	0.071	0.070	0.064	0.063	0.060	0.077	0.084	0.100	0.095	0.089	0.077	0.07

Table 2
The parameters used in the market co-equilibrium model.

Parameter	$\underline{\lambda}_{i,j}^{pro,ask}$	$\overline{\lambda}_{i,j}^{pro,ask}$	$\underline{x}_{i,*}^{DA}$	$\overline{x}_{i,*}^{network}$	R	T	β	γ
Value	0.04 (£/kWh)	0.04 (£/kWh)	10 kW	200 kW	8.314 (J/mol K)	300.15 K	0.05 (−)	0.1 (−)

$$\sum_{i=1}^{M}\sum_{j=1}^{N} f\left(\boldsymbol{x}_{i,j}^{*}\right) \geq \left\{ \sum_{i=1}^{M}\sum_{j=1}^{N} f\left(\boldsymbol{x}_{i,j}^{k}\right) + \sum_{i=1}^{M}\sum_{j=1}^{N} \frac{\partial f_{i,j}\left(\boldsymbol{x}_{i,j}^{k}\right)}{\partial x_{i,j}} \left(\boldsymbol{x}_{i,j}^{*} - \boldsymbol{x}_{i,j}^{k}\right) + \frac{1}{2}\sum_{i=1}^{M} \times \sum_{j=1}^{N} \gamma \left(\boldsymbol{x}_{i,j}^{*} - \boldsymbol{x}_{i,j}^{k}\right)^{2} \right\} \tag{19}$$

where γ is a positive constant. The corresponding feasible constraints of both sides can be added to both sides, which yields Augmented Lagrange functions. The Augmented Lagrange function is the sum of all prosumers. By applying the Augmented Lagrange function in Eq. (A.16), it can be obtained that:

$$\begin{aligned} L\left(x_{*j}^{*}, \mu_{x}^{*}, \mu_{z}^{*}, \lambda^{*}\right) &\geq L\left(x_{*j}^{k}, \mu_{x}^{k}, \mu_{z}^{k}, \lambda^{k}\right) \\ &+\frac{1}{2}\gamma\left\|x^{*} - x^{k}\right\|^{2} + \mathbb{I}^{T}\nabla_{x}L\left(x_{*j}^{k}, \mu_{x}^{k}, \mu_{z}^{k}, \lambda^{k}\right)\left(x_{ij}^{*} - x_{ij}^{k}\right)\mathbb{I} \end{aligned} \tag{20}$$

with

$$L\left(x, z, \mu_{x}^{*}, \mu_{z}^{*}, \lambda^{*}\right) \geq L\left(x^{*}, z^{*}, \mu_{x}^{*}, \mu_{z}^{*}, \lambda^{*}\right) \tag{21}$$

Then it can be derived to get:

$$\begin{aligned} L\left(x^{*}, \mu_{x}^{*}, \mu_{z}^{*}, \lambda^{*}\right) \geq argmin_{x} \Big\{ & L\left(x, \mu_{x}^{k}, \mu_{z}^{k}, \lambda^{k}\right) + \frac{1}{2}\gamma\left\|x - x^{k}\right\|^{2} \\ & +\mathbb{I}^{T}\nabla_{x}L\left(x^{k}, \mu_{x}^{k}, \mu_{z}^{k}, \lambda^{k}\right)\left(x - x^{k}\right)\mathbb{I} \end{aligned} \tag{22}$$

Table 3
The synthetic prosumers data.

Prosumer id	A (−)	z (−)	c (−)	$\bar{x}_{*,j}$ (kWh)	Prosumer id	A (−)	z (−)	c (−)	$\bar{x}_{*,j}$ (kWh)
1	0.305	0.705	110	7	30	0.193	0.593	590	3.6
2	0.18	0.58	90	3.6	31	0.323	0.723	250	3.6
3	0.157	0.557	80	3.6	32	0.102	0.502	630	7
4	0.311	0.711	330	3.6	33	0.28	0.68	90	3.6
5	0.24	0.64	450	7	34	0.111	0.511	560	7
6	0.182	0.582	240	3.6	35	0.108	0.508	640	7
7	0.266	0.666	130	3.6	36	0.262	0.662	340	7
8	0.221	0.621	440	7	37	0.203	0.603	530	3.6
9	0.258	0.658	370	7	38	0.243	0.643	590	3.6
10	0.137	0.537	380	3.6	39	0.117	0.517	260	3.6
11	0.109	0.509	460	3.6	40	0.135	0.535	490	7
12	0.333	0.733	540	7	41	0.253	0.653	540	3.6
13	0.231	0.631	560	3.6	42	0.191	0.591	100	7
14	0.334	0.734	150	7	43	0.234	0.634	570	7
15	0.259	0.659	420	7	44	0.321	0.721	240	3.6
16	0.167	0.567	70	7	45	0.13	0.53	490	7
17	0.209	0.609	370	3.6	46	0.197	0.597	520	7
18	0.259	0.659	630	7	47	0.201	0.601	60	7
19	0.289	0.689	570	3.6	48	0.194	0.594	400	3.6
20	0.207	0.607	360	7	49	0.15	0.55	320	7
21	0.33	0.73	190	7	50	0.181	0.581	340	7
22	0.139	0.539	190	3.6	51	0.193	0.593	500	3.6
23	0.142	0.542	490	7	52	0.266	0.666	600	7
24	0.259	0.659	290	7	53	0.188	0.588	600	3.6
25	0.249	0.649	560	3.6	54	0.346	0.746	170	7
26	0.31	0.71	590	3.6	55	0.237	0.637	460	3.6
27	0.225	0.625	100	7	56	0.182	0.582	140	3.6
28	0.273	0.673	560	7	57	0.335	0.735	630	7
29	0.155	0.555	150	7					

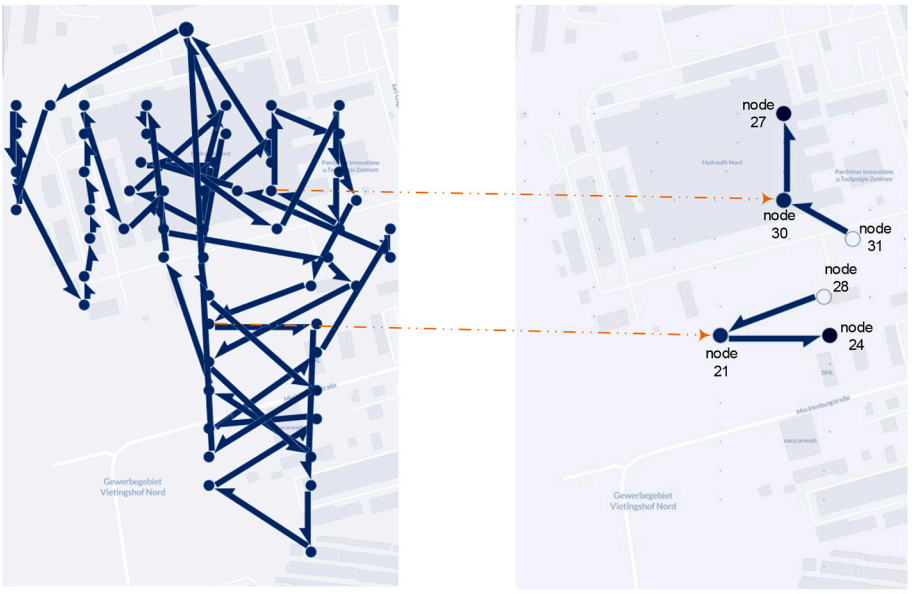

Fig. 6. Visualization of information flow in the network graph.

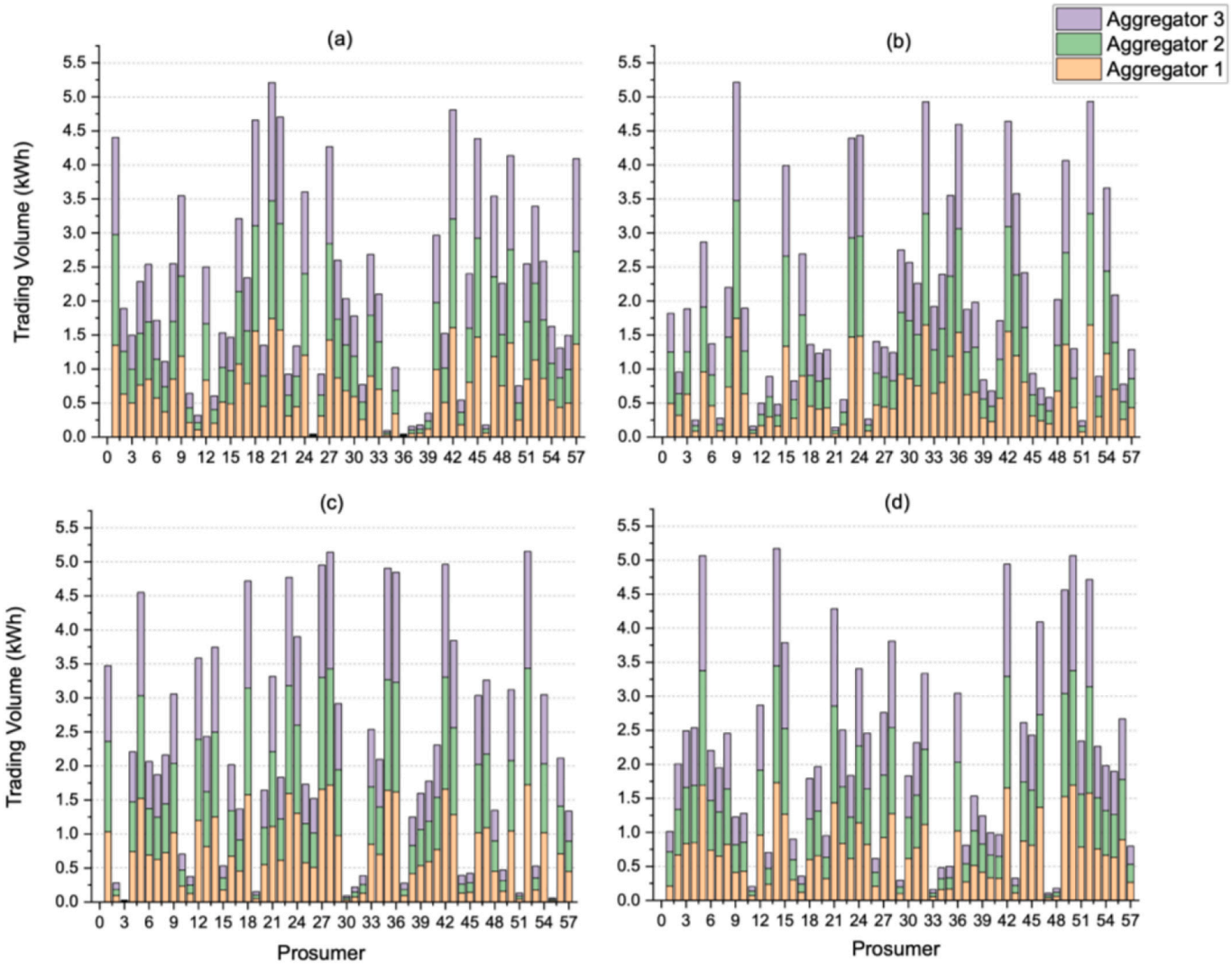

Fig. 7. Trading volume visualization (a) the trading volumes at 2 am; (b) the trading volumes at 8 am; (c) the trading volumes at 2 pm; (d) the trading volumes at 8 pm.

Then taking the derivative on the right gives:

$$\left\|\nabla_x L\left(x^k,\mu_x^k,\mu_z^k,\lambda^k\right)\right\|_2^2 \geq 2\gamma\left(L\left(x^k,\mu_x^k,\mu_z^k,\lambda^k\right)-L\left(x^*,\mu_x^*,\mu_z^*,\lambda^*\right)\right) \tag{23}$$

According to the convexity of Lagrangian Eq. (22), after substituting the convexity of prosumers' utility function, Eq. (24) can be derived:

$$\begin{aligned} L\left(x^k,\mu_x^k,\mu_z^k,\lambda^k\right) &\geq L\left(x^{k+1},\mu_x^{k+1},\mu_z^{k+1},\lambda^{k+1}\right)+\mathbb{I}^T\nabla_x L\left(x^{k+1},\mu_x^{k+1},\mu_z^{k+1},\lambda^{k+1}\right)^T\left(x^k-x^{k+1}\right)\mathbb{I} \\ &\geq L\left(x^{k+1},\mu_x^{k+1},\mu_z^{k+1},\lambda^{k+1}\right)+\sum_{i=1}^{M}\sum_{j=1}^{N}\left(\frac{\partial L\left(\left(x^{k+1},\mu_x^{k+1},\mu_z^{k+1},\lambda^{k+1}\right)\right)}{\partial_{x_{ij}}}\right)\times\frac{1}{k}\left(\frac{\partial L_j\left(x_{i,j}^k\right)}{\partial x_{i,j}}-\frac{\partial L_j\left(x_{i,j}^{k+1}\right)}{\partial x_{i,j}}\right) \end{aligned} \tag{24}$$

When k is sufficiently large, Eq. (18) and the Karush–Kuhn–Tucker conditions can be applied such that:

$$\frac{\partial L\left(x^{k+1},\mu_x^{k+1},\mu_z^{k+1},\lambda^{k+1}\right)}{\partial_{x_{ij}}}+\frac{\partial L_j\left(x_{i,j}^k\right)}{\partial x_{i,j}}-\frac{\partial L_j\left(x_{i,j}^{k+1}\right)}{\partial x_{i,j}}=0 \tag{25}$$

Combining Eqs. (24) and (25) into Eq. (23) yields:

$$\begin{aligned} L\left(x^k,\mu_x^k,\mu_z^k,\lambda^k\right) &\geq L\left(x^{k+1},\mu_x^{k+1},\mu_z^{k+1},\lambda^{k+1}\right) \\ &+2\frac{\gamma}{k}\left(L\left(x^k,\mu_x^k,\mu_z^k,\lambda^k\right)-L\left(x^*,\mu_x^*,\mu_z^*,\lambda^*\right)\right) \end{aligned} \tag{26}$$

Then reformulating Equitation (26) yields:

$$\frac{L\left(x^{k+1},\mu_x^{k+1},\mu_z^{k+1},\lambda^{k+1}\right)-L\left(x^*,\mu_x^*,\mu_z^*,\lambda^*\right)}{L\left(x^k,\mu_x^k,\mu_z^k,\lambda^k\right)-L\left(x^*,\mu_x^*,\mu_z^*,\lambda^*\right)}=\frac{1}{1+2\frac{\gamma}{k}}<1 \tag{27}$$

This allows the assertion that the proposed algorithm has a linear convergence rate.

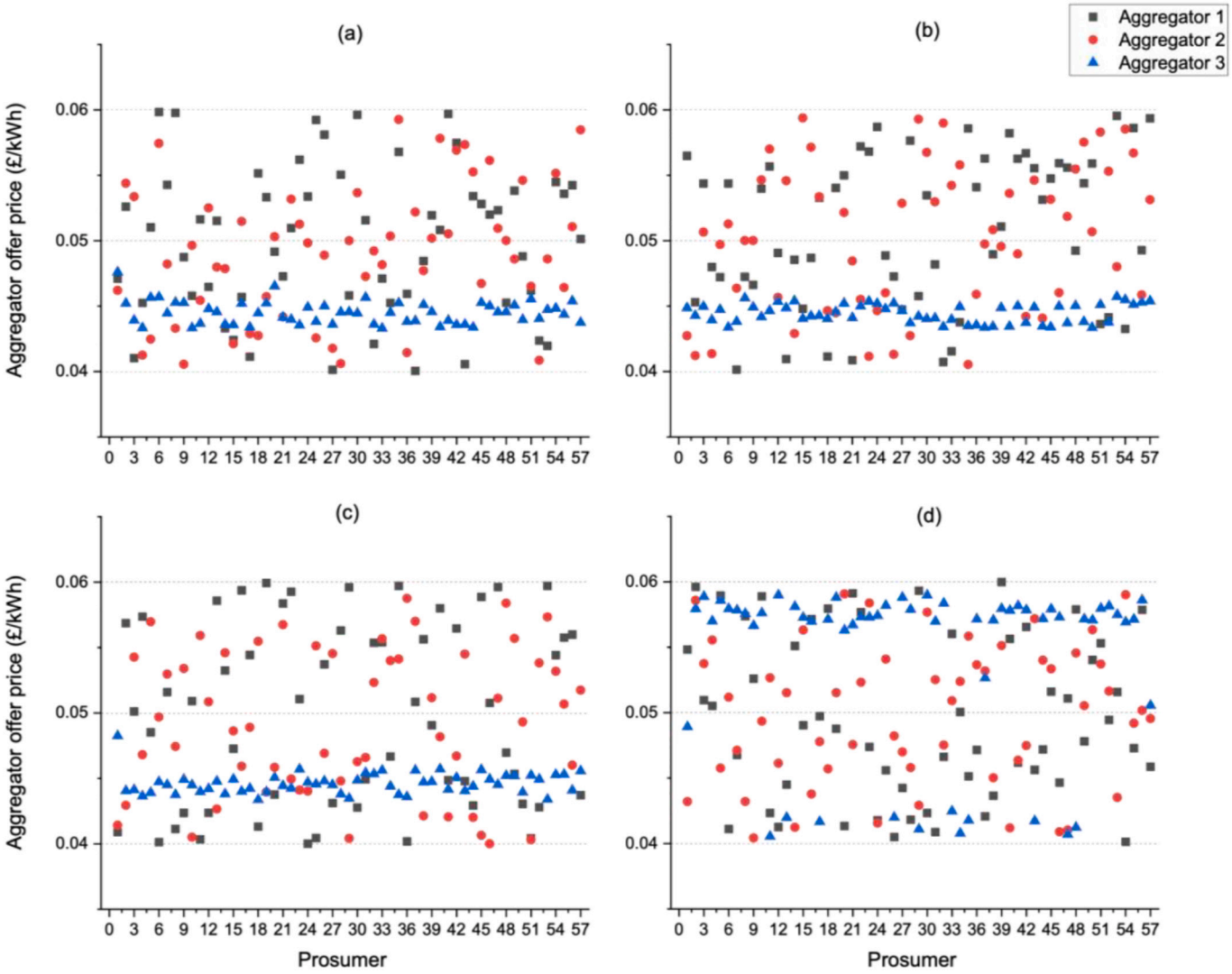

Fig. 8. Aggregator offer price visualization (a) the offer price at 2 am; (b) the offer price at 8 am; (c) the offer price at 2 pm; (d) the offer price at 8 pm.

Table 4
Comparison of the proposed algorithm with the benchmarks.

Name	Communication Complexity	Convergence Rate	Privacy Preserving	Graph Structure
Classical ADMM [39]	$O\left(ln\left(\frac{1}{\epsilon}\right).\mathrm{P}^3\right)$	Linear	No	Complete
Walkman ADMM [45]	$O\left(ln\left(\frac{1}{\epsilon}\right).\frac{\mathrm{P}ln^3(\mathrm{P})}{(1-\rho_{\max}(\mathrm{Q}))^2}\right)$	Linear	Yes	Random
RW-ADMM [48]	$O\left(ln\left(\frac{1}{\epsilon}\right).\frac{\mathrm{E}^2}{\mathrm{P}\sqrt{1-\rho_{\max}(\mathrm{Q})}}\right)$	Linear	Yes	Fixed subgraph
Proposed algorithm	$O\left(ln\left(\frac{1}{\epsilon}\right).\mathrm{P}^2\right)$	Linear	Yes	Cycle

3. Intelligent aggregation application

In this section, the intelligent aggregation architecture is applied with an example of a low voltage (LV) to medium voltage (MV) distribution network with synthetic prosumer data.

3.1. Experiment setup

This case study is based on the open-source electric network benchmark database named Simbench [47]. The Simbench data is generated by clustering the publicly available electric network data in Germany. We chose an urban LV distribution network benchmark data from the Simbench database. The benchmark LV distribution network consists of 59 buses, and we modified the bus data to incorporate 57 hypothetical prosumers with 5 PV units with a 5 kW power rating and 57 EVs. The modified distribution network is shown in Fig. 5. All EVs are assumed to be able to have V2G capabilities. In this example, both PV and EV units are modelled as static generators.

The day-ahead prices used in this case study are obtained from the Nord Pool UK day-ahead price [48], shown in Table 1. This study selects

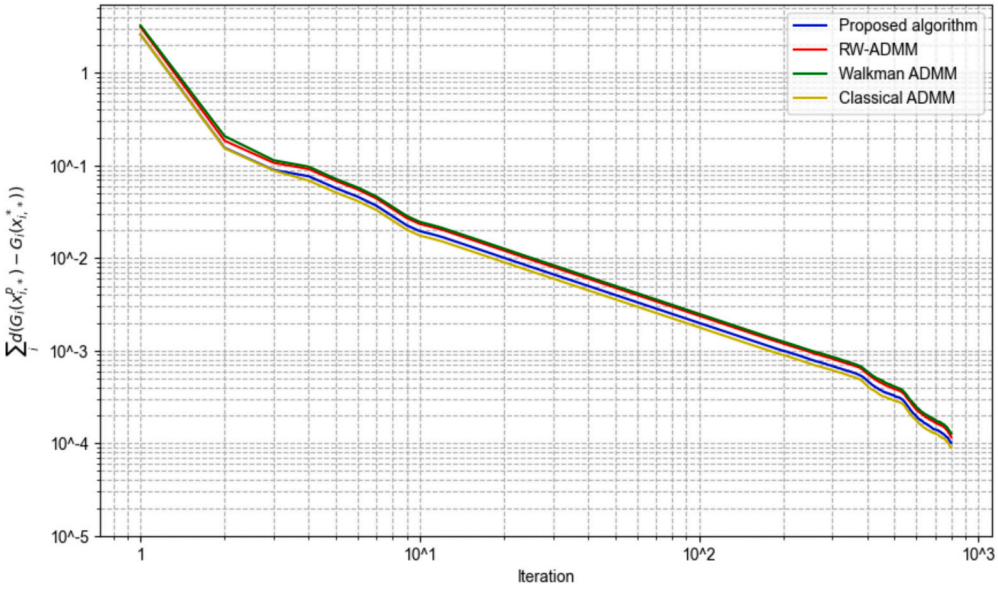

Fig. 9. Comparison of convergence rate between the proposed algorithm and the benchmarks.

the 2nd, 8th, 14th and 20th hour for the day-ahead market price. Table 2 shows the parameters used in the market co-equilibrium model, and Table 3 shows the detailed case study data for the 57 synthetic prosumers.

3.2. Results and discussion

The shortest Hamiltonian communication path was constructed for communicating between neighboring prosumers. For demonstration, a front-end web[2] was developed to show the Hamiltonian communication path of 57 prosumers, which can be extended to monitor real-time optimization and information flow sharing. Each prosumer can share their information with their neighbors in the network graph to reach a consensus state. Fig. 6 demonstrates how the information is shared in the network graph. The network graph is plotted with the geo-tag data provided by Simbench. In Fig. 6(a), the information flow during the optimization process is demonstrated, where the nodes in the network construct a Hamiltonian path. In Fig.6 (b), subgraphs of node 21 and node 30 were highlighted to indicate the information flow. For subgraph x_{21}, the trading volume information is passed from node 28. Once node 21 optimizes the local objective function, the trading volume information is passed to node 24. A similar information flow can also be observed in the subgraph x_{30}, where node 30 optimizes the information provided by node 31. Then, node 30 sends the optimized results to node 27.

The result of the aggregation volume of 57 prosumers is shown in Fig. 7, which is the optimized result of the trading volume matrix $\boldsymbol{X}$ for the lower-level game. There is a considerable trading volume variance among prosumers due to the differences in their energy assets. The differences include the maximum discharge rating of batteries, as well as the health of the batteries. For example, prosumer 37 has an aged battery ($c = 530$) and a low battery discharge bound ($\overline{x}_{*,37}$=3.6kWh). It is worth noting that the trading volume at night is less than that during the day, which reflects a reasonable game result, i.e., prosumers tend to sell their surplus electricity during the day and charge it at nighttime, because electricity prices are usually higher at the daytime. In addition to the trading volume, Fig. 8 shows the game result for the upper-level game, where each aggregator competes with each other by determining the aggregation offer price $\lambda_{i,j}^{pro,ask}$. It can be seen from the figure that the price offered to prosumers varied considerably among aggregators. For instance, aggregator 1, aggregator 2, and aggregator 3 offer to pay 0.044, 0.055, 0.043 £/kWh, respectively, to prosumer 52 at 8 am to aggregate the electricity. As a result, prosumer 52 receive £0.217 from three prosumers. Subsequently, aggregators make £0.092, £0.0914, and £0.0919, respectively, to facilitate the aggregation. Thus, aggregators are able to profit by providing aggregation facilitation services. In addition, the profits of aggregators will increase with more prosumers participating in the aggregation process. The following section will conduct a benchmark analysis to prove the effectiveness of our proposed algorithm.

3.3. Benchmark analysis

Table 4 shows the comparison of the proposed algorithm with the benchmarks, including Classical ADMM [39], Walkman ADMM [45], and RW-ADMM [48]. Following the same notation in section 2.1.2, P, E are represented as the total nodes and edges in a graph, where E is an integer in the range of $[\mathrm{P}, \mathrm{P}(\mathrm{P}-1)]$. Q is denoted as the edge connection matrix, and $\rho_{\max}(\mathrm{Q})$ is the largest eigenvalue of the connection matrix. According to the proof [49], the multi-block ADMM can achieve a linear convergence rate in convex problems. Therefore, basic ADMM and its variants can achieve a linear convergence rate. If the bounded error of an optimization method with a linear convergence rate is expected to be within $(0, \epsilon)$, the iteration time is to $O\left(ln\left(\frac{1}{\epsilon}\right)\right)$ [50]. The comparison of convergence rate between the proposed algorithm and the benchmarks is shown in Fig. 9. The proposed algorithm exhibits a linear convergence rate consistent with the benchmarks.

Since all convergence rates are linear, merely measuring the convergence rate is not enough. Another criterion for evaluating the performance of distributed algorithms is communication complexity because graph structures have different communication costs. The graph structure can be divided into four types, complete [39], random [45], fixed subgraph [48], and cycle [51]. The complete cannot preserve the private information of prosumers since all data will be shared. Random, fixed subgraphs and cycles can preserve privacy when optimizing. According to the graph theory [51] and computation method in [45], the classical ADMM in a complete graph has a communication complexity as $O\left(ln\left(\frac{1}{\epsilon}\right).\mathrm{P}^3\right)$, with the communication complexity. Walkman ADMM

[2] https://tinyurl.com/3vv8ptzh

[45] and RW-ADMM [48] have a better performance, with $O\left(ln\left(\frac{1}{\epsilon}\right).\frac{Pln^3(P)}{(1-\rho_{max}(Q))^2}\right)$ and $O\left(ln\left(\frac{1}{\epsilon}\right).\frac{E^2}{P\sqrt{1-\rho_{max}(Q)}}\right)$. When Hamiltonian path P is cyclic, the $1-\rho_{max}(Q) = O\left(1-cos\frac{2\pi}{P}\right) = O\left(\frac{1}{P^2}\right)$. In such a situation, our method can achieve a communication complexity as $O\left(ln\left(\frac{1}{\epsilon}\right).\frac{P}{\sqrt{1-\rho_{max}(Q)}}\right) = O\left(ln\left(\frac{1}{\epsilon}\right).P^2\right)$ according to [45]. When P is large but not limited to infinite, our method has lower complexity than the Walkman and RW-ADMM. When P is limited to infinite, the Walkman can be more communication efficient as $\lim_{P\to\infty} ln^3(P) \ll \lim_{P\to\infty} P$. For the aggregator trading problem in a community, the scale of optimization is usually a limited number of prosumers, so our method can be considered more efficient.

4. Conclusions

The penetration of DER and IoT technologies is transforming power systems' generation, transmission, consumption, and decision-making. The power flow has transitioned to bidirectional rather than unidirectional but hierarchical control has not changed. Moreover, decentralized decision-making architecture is emerging to challenge the traditional centralized one in order to ensure data privacy and security and to allow prosumers to optimize their utility. Thus, this paper proposes an intelligent aggregation architecture to facilitate a more sophisticated energy transition. The architecture adopts edge computing technologies to compute a MLMFG model with a novel graph-based consensus algorithm. This study proved the existence and uniqueness of the MLMFG model and convergence analysis of the proposed algorithm with a systematic convex approach. In addition, this study examined the applicability of the proposed intelligent aggregation framework on a distribution network, where the results showed the competitive game relationship among the aggregators. With a benchmark analysis, the proposed algorithm is compared with the state-of-the-art algorithm in terms of communication complexity, privacy preservation, and convergence rate. It is shown that the proposed algorithm has a communication complexity of $O\left(ln\left(\frac{1}{\epsilon}\right).P^2\right)$, which means the proposed algorithm performs better than state-of-the-art algorithms in terms of communication complexity.

Future work could focus on inter-temporal decision-making and contractual agreement in electricity aggregation. The optimal strategy of the aggregation process could consider prosumers' decisions on electricity storage. The prosumers with storage units could store energy when the electricity price is low and sell stored electricity when the price is high. The optimal strategy requires inter-temporal decision-making. Moreover, the contractual agreement between prosumers and aggregators requires further research. In the conventional energy system, the contractual agreement of generation, transmission, and distribution are centralized by involved companies. In the decentralized energy system, the contractual agreements between agents are dynamic and hard to enforce. Blockchain technology could be a viable solution to establish contractual agreements among decentralized agents.

Declaration of competing interest

The authors declare that they have no known competing financial interests or personal relationships that could have appeared to influence the work reported in this paper.

The authors declare no competing interest.

Data availability

Data will be made available on request.

Acknowledgements

This work was supported by the Engineering and Physical Sciences Research Council project (EP/S003088/1) 'Aggregators as diGital Intermediaries in Local Electricity markets' (AGILE) and (EP/V054082/1) 'Data Analytics Facility for National Infrastructure' (DAFNI).

Appendix A. Market Equilibrium Proof

A.1. The existence and uniqueness of optimal solution

The existence and uniqueness of the optimal solution ensures that the aggregation process will reach a co-equilibrium state where the utility values of both aggregators and prosumers are optimal. $\boldsymbol{\chi}$ ***and*** $\boldsymbol{\Lambda}$ are defined as the closed convex feasible sets of aggregate volume matrix $\boldsymbol{X} \in \mathbb{R}^{\boldsymbol{M}\times\boldsymbol{N}}$ and ask price matrix $\boldsymbol{\Lambda} \in \mathbb{R}^{\boldsymbol{M}\times\boldsymbol{N}}$, respectively. A point $(\mathbf{X}^*, \boldsymbol{\Lambda}^*) \in (\chi, \boldsymbol{\Lambda})$ is the bi-level optimum solution if it can meet the two inequality requirements (A.1) simultaneously:

$$\sum_{j=1}^{N}\left(\lambda_i^{DA,bid} - \lambda_{i,j}^{pro,ask^*}\right)x_{i,j} > \sum_{j=1}^{N}\left(\lambda_i^{DA,bid} - \lambda_{i,j}^{pro,ask}\right)x_{i,j} \tag{A.1}$$

$$\sum_{i=1}^{M}\lambda_{i,j}^{pro}x_{*j}^{*} - \mathbb{I}^T Ae^{\left(\frac{\beta x_{*j}^{*}}{RT}\right)}c^z + \mathbb{I}^T\frac{\partial Ae^{\left(\frac{\beta x_{*j}^{*}}{RT}\right)}c^z}{\partial x_{i,j}} > \sum_{i=1}^{M}\lambda_{i,j}^{pro}x_{*j} - \mathbb{I}^T Ae^{\left(\frac{\beta x_{*j}}{RT}\right)}c^z + \mathbb{I}^T\frac{\partial Ae^{\left(\frac{\beta x_{*j}}{RT}\right)}c^z}{\partial x_{i,j}}$$

Before proving the optimal point exists in MLMFG, the following notation is introduced to enhance the readability of the proof. Eq. (A.2) and (A.3) represent the second and third terms of the prosumers' utility functions. $L_j(x_{*j})$ is close and convex with the minimum feasible solution. $\theta_j(x_{*j})$ can be regarded as the first-order derivative of Eq. (A.2), $\theta_j(x_{*j}) = \frac{\partial L_j(x_{*j})}{\partial x_{i,j}}$.

$$L_j(x_{*j}) = Ae^{\left(\frac{\beta x_{*j}}{RT}\right)}c^z \tag{A.2}$$

$$\theta_j\left(x_{*j}\right)=\frac{\partial x_{*j} A e^{\left(\frac{\beta x_{*j}}{RT}\right)} c^z}{\partial x_{i,j}} \tag{A.3}$$

Assumption 1. The utility function of each prosumer should be satisfied with the Lipschitz gradient continuity. There exists an upper bound value k satisfying that:

$$\nabla_{x_{*j}}\left\{\sum_{i=1}^{M}\lambda_{i,j}^{pro}x_{*j}^{k+1}-\mathbb{I}^T L_j\left(x_{*j}^{k+1}\right)\right\}-\nabla_{x_{*j}}\left\{\sum_{i=1}^{M}\lambda_{i,j}^{pro}x_{*j}^{k}-\mathbb{I}^T L_j\left(x_{*j}^{k}\right)\right\}\preccurlyeq k\left(x_{*j}^{k+1}-x_{*j}^{k}\right) \tag{A.4}$$

where $\nabla_{x_{*j}}$ is the first-order differential operator. A≼B means A − B is at least a positive semi-definite matrix. Proof.

Converting the concave function of the optimization problem represented by (3) and (4) in MLMFG to a convex function can respectively obtain the upper-level optimization problem represented by (A.5) and the lower-level optimization problem represented by (A.6). (A.5.a) is a general representation of the constraints of aggregators (3.a). Similarly, (A.6.a) represents the constraints of prosumers (4.a) and (4.b).

Aggregator's optimization problem:

$$\underset{\lambda_{i,*}^{pro}}{argmin}-\sum_{j=1}^{N}\left(\lambda_i^{DA,bid}-\lambda_{i,j}^{pro,ask}\right)x_{i,j},i=1,2,\ldots M \tag{A.5}$$

$$s.t.c_a\left(\lambda_{i,*}^{pro}\right)\in C_a,a=1,2,\ldots A \tag{A.5.a}$$

Prosumer's optimization problem:

$$\underset{x_{*j}}{arg\,min}-\sum_{i=1}^{M}\lambda_{i,j}^{pro}x_{i,j}+\mathbb{I}^T L_j\left(x_{*j}\right)-\mathbb{I}^T\theta_j\left(x_{*j}\right),j=1,2,\ldots N \tag{A.6}$$

$$s.t.d_b\left(x_{*j}\right)\in D_b,b=1,2,\ldots B \tag{A.6.a}$$

The inner loop in MLMFG can be regarded as an optimization problem with a Gauss-Seidel ADMM. It should be noted that the *aggregator*$_i$'s payment to *prosumer*$_j$, $\lambda_{i,j}^{pro}$ are fixed during the inner loop.

$$\underset{x_{*j}}{arg\,min}-\sum_{i=1}^{M}\lambda_{i,j}^{pro}x_{i,j}+\mathbb{I}^T L_j\left(x_{*j}\right)-\mathbb{I}^T\theta_j\left(x_{*j}\right),j=1,2,\ldots N \tag{A.7}$$

$$\mathrm{s.t.}\mathbb{I}_{C_a}\left(\lambda_{i,*}^{pro}\right),a=1,2,\ldots A$$

$$\mathrm{s.t.}\mathbb{I}_{D_b}\left(x_{*j}\right),b=1,2,\ldots B$$

The lower-level optimization problem (A.7) can then be transferred to the augmented Lagrange function with $\mu_x=\left[\mu_1^x,\mu_2^x,\ldots,\mu_p^x\right]$ and $\mu_z=\left[\mu_1^y,\mu_2^y,\ldots,\mu_q^y\right]$ as Langrangian multipliers for inequality constraints:

$$x_{*j}^{k+1}=\underset{x_{*j}}{arg\,min}\ L_0\left(x_{*j},\mu_x^*,\mu_z^*,\lambda^*\right) \tag{A.8}$$

Based on the **Assumption 1**, the utility function reaches the optimal value when $\frac{\partial L_o\left(x_{*j},\mu_x^*,\mu_z^*,\lambda^*\right)}{\partial x_{i,j}}=0$. Thus, for any index pair i and j at the $k+1$ step, Eq. (A.9) is obtained:

$$-\frac{\partial\lambda_{i,j}^{pro}x_{*j}^{k+1}}{\partial x_{i,j}}+\frac{\partial L_j\left(x_{*j}^{k+1}\right)}{\partial x_{i,j}}-\frac{\partial L_j\left(x_{*j}^{k}\right)}{\partial x_{i,j}}+\frac{\partial\mu_{x,j}^{k+1}\left(\mathbb{I}_{D_b}\left(x_{*j}^{k+1}\right)\right)}{\partial x_{i,j}}+\frac{\partial\frac{\rho}{2}\left\|\mathbb{I}_{D_b}\left(x_{*j}^{k+1}\right)\right\|}{\partial x_{i,j}}=0 \tag{A.9}$$

It has been proved that the inequality-constrained-ADMM can restrict the solution projected into the feasible domain of the indicator function. When k is sufficiently large, the gradient of the indicator functions can be zero. When the gradients of the indicator function vanish, then we can obtain the Eq. (A.10):

$$\frac{\partial\lambda_{i,j}^{pro}x_{*j}^{k+1}}{\partial x_{i,j}}=\frac{\partial L_j\left(x_{*j}^{k+1}\right)}{\partial x_{i,j}}-\frac{\partial L_j\left(x_{*j}^{k}\right)}{\partial x_{i,j}} \tag{A.10}$$

$\left(x_{i,j}^{k+1}-x_{i,j}^{k}\right)$ can be multiplied by both sides of Eq. (A.10) to obtain the Eq. (A.11):

$$\frac{\partial\lambda_{i,j}^{pro}x_{*j}^{k+1}}{\partial x_{i,j}}\left(x_{i,j}^{k+1}-x_{i,j}^{k}\right)=\left(\frac{\partial L_j\left(x_{i,j}^{k+1}\right)}{\partial x_{i,j}}-\frac{\partial L_j\left(x_{i,j}^{k}\right)}{\partial x_{i,j}}\right)\left(x_{i,j}^{k+1}-x_{i,j}^{k}\right) \tag{A.11}$$

Based on the variational inequality in [52], Eq. (A.12) can be inferred.

$$\left(\frac{\partial L_j\left(x_{i,j}^{k+1}\right)}{\partial x_{i,j}}-\frac{\partial L_j\left(x_{i,j}^{k}\right)}{\partial x_{i,j}}\right)\left(x_{i,j}^{k+1}-x_{i,j}^{k}\right)\geq 0 \tag{A.12}$$

Then

$$\frac{\partial \lambda_{i,j}^{pro} x_{i,j}^{k+1}}{\partial x_{i,j}}\left(x_{i,j}^{k+1}-x_{i,j}^{k}\right)\geq 0 \tag{A.13}$$

Therefore

$$\sum_{i=1}^{M}\sum_{j=1}^{N}\frac{\partial \lambda_{i,j}^{pro} x_{i,j}^{k+1}}{\partial x_{i,j}}\left(x_{i,j}^{k+1}-x_{i,j}^{k}\right)\geq 0 \tag{A.14}$$

Recall first-order Taylor series of convexity of functions with **Assumption 1**:

$$f(x+p)\approx f(x)+\partial f(x)p \tag{A.15}$$

where $p\to 0$, expand the function $\sum_{i=1}^{M}\sum_{j=1}^{N} f\left(x_{i,j}^{k+1}\right)$ into the optimization problem when $x_{i,j}^{k+1}\to x_{i,j}^{k}$:

$$\sum_{i=1}^{M}\sum_{j=1}^{N}\lambda_{i,j}^{pro} x_{i,j}^{k+1}=\sum_{i=1}^{M}\sum_{j=1}^{N}\lambda_{i,j}^{pro} x_{i,j}^{k}+\sum_{i=1}^{M}\sum_{j=1}^{N}\frac{\partial \lambda_{i,j}^{pro} x_{i,j}^{k+1}}{\partial x_{i,j}}\left(x_{i,j}^{k+1}-x_{i,j}^{k}\right) \tag{A.16}$$

It can be concluded that:

$$\sum_{i=1}^{M}\sum_{j=1}^{N}\lambda_{i,j}^{pro} x_{i,j}^{k+1}\geq\sum_{i=1}^{M}\sum_{j=1}^{N}\lambda_{i,j}^{pro} x_{i,j}^{k} \tag{A.17}$$

Eq. (A.17) means the revenue of prosumers increases along the vector field. Since the lower-level game is convex and bounded, the optimum of the lower-level game can be achieved. In addition, the upper-level game is linear and bounded, and it can also reach the optimum when the lower-level optimum is achieved. In other words, leader's and follower's game can reach the global optimum if taking sufficient iteration steps. More precisely, from the variational inequality Proposition 2.6 in [53], convergence will reach the equilibrium point with:

$$\left\langle\begin{pmatrix}\nabla_{x_{*,1}}\sum_{j=1}^{N}\lambda_{i,j}^{pro}x_{i,j}^{k}\\ \vdots\\ \nabla_{x_{*,N-1}}\sum_{j=1}^{N}\lambda_{i,j}^{pro}x_{i,j}^{k}\\ \nabla_{x_{*,N}}\sum_{j=1}^{N}\lambda_{i,j}^{pro}x_{i,j}^{k}\end{pmatrix},\begin{pmatrix}x_{*,1}^{k+1}-x_{*,1}^{k}\\ \vdots\\ x_{*,N-1}^{k+1}-x_{*,N-1}^{k}\\ x_{*,N}^{k+1}-x_{*,N}^{k}\end{pmatrix}\right\rangle\leq 0 \tag{A.18}$$

Equitation (A.18) can be set as a stopping criterion of convergence.

References

[1] Guerrero J, Gebbran D, Mhanna S, Chapman AC, Verbič G. Towards a transactive energy system for integration of distributed energy resources: home energy management, distributed optimal power flow, and peer-to-peer energy trading. Renew Sust Energ Rev 2020:132. https://doi.org/10.1016/j.rser.2020.110000.

[2] Soto EA, Bosman LB, Wollega E, Leon-Salas WD. Peer-to-peer energy trading: a review of the literature. Appl Energy 2021:283. https://doi.org/10.1016/j.apenergy.2020.116268.

[3] Jain RK, Qin J, Rajagopal R. Data-driven planning of distributed energy resources amidst socio-technical complexities. Nat Energy 2017:2. https://doi.org/10.1038/nenergy.2017.112.

[4] Noori M, Zhao Y, Onat NC, Gardner S, Tatari O. Light-duty electric vehicles to improve the integrity of the electricity grid through vehicle-to-grid technology: analysis of regional net revenue and emissions savings. Appl Energy 2016;168:146–58. https://doi.org/10.1016/j.apenergy.2016.01.030.

[5] Jin J, Gubbi J, Marusic S, Palaniswami M. An information framework for creating a smart city through internet of things. IEEE Internet Things J 2014;1:112–21. https://doi.org/10.1109/JIOT.2013.2296516.

[6] Pan J, McElhannon J. Future edge cloud and edge computing for internet of things applications. IEEE Internet Things J 2018;5:439–49. https://doi.org/10.1109/JIOT.2017.2767608.

[7] Xiong Z, Kang J, Niyato D, Wang P, Poor HV. Cloud/edge computing Service Management in Blockchain Networks: multi-leader multi-follower game-based ADMM for pricing. IEEE Trans Serv Comput 2020;13:356–67. https://doi.org/10.1109/TSC.2019.2947914.

[8] Tushar W, Yuen C, Saha TK, Morstyn T, Chapman AC, Alam MJE, et al. Peer-to-peer energy systems for connected communities: a review of recent advances and emerging challenges. Appl Energy 2021;282:116131. https://doi.org/10.1016/j.apenergy.2020.116131.

[9] Shabanzadeh M, Sheikh-El-Eslami MK, Haghifam MR. A medium-term coalition-forming model of heterogeneous DERs for a commercial virtual power plant. Appl Energy 2016;169:663–81. https://doi.org/10.1016/j.apenergy.2016.02.058.

[10] Jafari M, Akbari Foroud A. A medium/long-term auction-based coalition-forming model for a virtual power plant based on stochastic programming. Int J Electr Power Energy Syst 2020:118. https://doi.org/10.1016/j.ijepes.2019.105784.

[11] Rahimiyan M, Baringo L. Strategic bidding for a virtual power Plant in the day-Ahead and Real-Time Markets: a Price-taker robust optimization approach. IEEE Trans Power Syst 2016;31:2676–87. https://doi.org/10.1109/TPWRS.2015.2483781.

[12] Kardakos EG, Simoglou CK, Bakirtzis AG. Optimal offering strategy of a virtual power plant: a stochastic bi-level approach. IEEE Trans Smart Grid 2016;7:794–806. https://doi.org/10.1109/TSG.2015.2419714.

[13] Tajeddini MA, Rahimi-Kian A, Soroudi A. Risk averse optimal operation of a virtual power plant using two stage stochastic programming. Energy 2014;73:958–67. https://doi.org/10.1016/j.energy.2014.06.110.

[14] Wang H, Riaz S, Mancarella P. Integrated techno-economic modeling, flexibility analysis, and business case assessment of an urban virtual power plant with multi-market co-optimization. Appl Energy 2020:259. https://doi.org/10.1016/j.apenergy.2019.114142.

[15] Naval N, Yusta JM. Virtual power plant models and electricity markets - a review. Renew Sust Energ Rev 2021:149. https://doi.org/10.1016/j.rser.2021.111393.

[16] Edmunds C, Galloway S, Dixon J, Bukhsh W, Elders I. Hosting capacity assessment of heat pumps and optimised electric vehicle charging on low voltage networks. Appl Energy 2021:298. https://doi.org/10.1016/j.apenergy.2021.117093.
[17] Alahyari A, Ehsan M, Mousavizadeh MS. A hybrid storage-wind virtual power plant (VPP) participation in the electricity markets: a self-scheduling optimization considering price, renewable generation, and electric vehicles uncertainties. J Energy Storage 2019:25. https://doi.org/10.1016/j.est.2019.100812.
[18] Rahimiyan M, Baringo L. Strategic bidding for a virtual power Plant in the day-Ahead and Real-Time Markets: a Price-taker robust optimization approach. IEEE Trans Power Syst 2016;31:2676–87. https://doi.org/10.1109/TPWRS.2015.2483781.
[19] Dabbagh SR, Sheikh-El-Eslami MK. Risk-based profit allocation to DERs integrated with a virtual power plant using cooperative game theory. Electr Power Syst Res 2015;121:368–78. https://doi.org/10.1016/j.epsr.2014.11.025.
[20] Zamani AG, Zakariazadeh A, Jadid S. Day-ahead resource scheduling of a renewable energy based virtual power plant. Appl Energy 2016;169:324–40. https://doi.org/10.1016/j.apenergy.2016.02.011.
[21] Zamani AG, Zakariazadeh A, Jadid S, Kazemi A. Stochastic operational scheduling of distributed energy resources in a large scale virtual power plant. Int J Electr Power Energy Syst 2016;82:608–20. https://doi.org/10.1016/j.ijepes.2016.04.024.
[22] Kardakos EG, Simoglou CK, Bakirtzis AG. Optimal offering strategy of a virtual power plant: a stochastic bi-level approach. IEEE Trans Smart Grid 2016;7:794–806. https://doi.org/10.1109/TSG.2015.2419714.
[23] Shafiekhani M, Badri A, Shafie-khah M, Catalão JPS. Strategic bidding of virtual power plant in energy markets: a bi-level multi-objective approach. Int J Electr Power Energy Syst 2019;113:208–19. https://doi.org/10.1016/j.ijepes.2019.05.023.
[24] Wei C, Xu J, Liao S, Sun Y, Jiang Y, Ke D, et al. A bi-level scheduling model for virtual power plants with aggregated thermostatically controlled loads and renewable energy. Appl Energy 2018;224:659–70. https://doi.org/10.1016/j.apenergy.2018.05.032.
[25] Nosratabadi SM, Hooshmand RA, Gholipour E. Stochastic profit-based scheduling of industrial virtual power plant using the best demand response strategy. Appl Energy 2016;164:590–606. https://doi.org/10.1016/j.apenergy.2015.12.024.
[26] Iria J, Soares F. An energy-as-a-service business model for aggregators of prosumers. Appl Energy 2023:347. https://doi.org/10.1016/j.apenergy.2023.121487.
[27] Obi M, Slay T, Bass R. Distributed energy resource aggregation using customer-owned equipment: a review of literature and standards. Energy Rep 2020;6:2358–69. https://doi.org/10.1016/j.egyr.2020.08.035.
[28] Okur Ö, Heijnen P, Lukszo Z. Aggregator's business models in residential and service sectors: a review of operational and financial aspects. Renew Sust Energ Rev 2021:139. https://doi.org/10.1016/j.rser.2020.110702.
[29] Iria J, Scott P, Attarha A, Gordon D, Franklin E. MV-LV network-secure bidding optimisation of an aggregator of prosumers in real-time energy and reserve markets. Energy 2022:242. https://doi.org/10.1016/j.energy.2021.122962.
[30] Shomalzadeh K, Scherpen JMA, Camlibel MK. Bilevel aggregator-prosumers' optimization problem in real-time: a convex optimization approach. Oper Res Lett 2022;50:568–73. https://doi.org/10.1016/j.orl.2022.08.008.
[31] Hu M, Fukushima M. Multi-leader-follower games: models, methods, and applications. J Oper Res Soc Jpn 2015;58:1–23.
[32] Nash JF. Equilibrium points in n-person games. Proc Natl Acad Sci 1950;36:48–9. https://doi.org/10.1073/pnas.36.1.48.
[33] Xiao Y, Xiao Y, Wang X, Pinson P, Wang X. Transactive energy based aggregation of prosumers as a retailer. IEEE Trans Smart Grid 2020;11:3302–12. https://doi.org/10.1109/TSG.2020.2976130.
[34] Hong Q, Meng F, Liu J, Bo R. A bilevel game-theoretic decision-making framework for strategic retailers in both local and wholesale electricity markets. Appl Energy 2023:330. https://doi.org/10.1016/j.apenergy.2022.120311.
[35] Sirojan T, Lu S, Phung BT, Ambikairajah E. Embedded edge computing for real-time smart meter data analytics. In: 2019 international conference on smart energy systems and technologies (SEST). IEEE; 2019. p. 1–5. https://doi.org/10.1109/SEST.2019.8849012.
[36] Aussel D, Svensson A. A short state of the art on multi-leader-follower games. In: Dempe S, Zemkoho A, editors. Bilevel optimization: Advances and next challenges. Cham: Springer International Publishing; 2020. p. 53–76. https://doi.org/10.1007/978-3-030-52119-6_3.
[37] Burger S, Chaves-Ávila JP, Batlle C, Pérez-Arriaga IJ. A review of the value of aggregators in electricity systems. Renew Sust Energ Rev 2017;77:395–405. https://doi.org/10.1016/j.rser.2017.04.014.
[38] Liu C, Wang Y, Chen Z. Degradation model and cycle life prediction for lithium-ion battery used in hybrid energy storage system. Energy 2019;166:796–806. https://doi.org/10.1016/j.energy.2018.10.131.
[39] Boyd S, Parikh N, Chu E, Peleato B, Eckstein J. Distributed optimization and statistical learning via the alternating direction method of multipliers. Foundations and Trends in Machine Learning 2010;3:1–122. https://doi.org/10.1561/2200000016.
[40] Giesen J, Laue S. Distributed convex optimization with many convex constraints. 2016.
[41] Rahman MS, Kaykobad M. On hamiltonian cycles and hamiltonian paths. Inf Process Lett 2005;94:37–41. https://doi.org/10.1016/j.ipl.2004.12.002.
[42] Oltean M. Solving the Hamiltonian path problem with a light-based computer. Nat Comput 2008;7:57–70. https://doi.org/10.1007/s11047-007-9042-z.
[43] Ye Y, Chen H, Ma Z, Xiao M. Decentralized consensus optimization based on parallel random walk. IEEE Commun Lett 2020;24:391–5. https://doi.org/10.1109/LCOMM.2019.2955442.
[44] Mota JFC, Xavier JMF, Aguiar PMQ, Püschel M. D-ADMM: a communication-efficient distributed algorithm for separable optimization. IEEE Trans Signal Process 2013;61:2718–23. https://doi.org/10.1109/TSP.2013.2254478.
[45] Mao X, Yuan K, Hu Y, Gu Y, Sayed AH, Walkman Yin W. A Communication-Efficient Random-Walk Algorithm for Decentralized Optimization. 2018.
[46] Makhdoumi A, Ozdaglar A. Convergence rate of distributed ADMM over networks. IEEE Trans Autom Control 2017;62:5082–95. https://doi.org/10.1109/TAC.2017.2677879.
[47] Meinecke S, Sarajlić D, Drauz SR, Klettke A, Lauven LP, Rehtanz C, et al. SimBench-A benchmark dataset of electric power systems to compare innovative solutions based on power flow analysis. Energies (Basel) 2020:13. https://doi.org/10.3390/en13123290.
[48] Shah SM, Avrachenkov KE. Linearly convergent asynchronous distributed ADMM via Markov sampling. 2018.
[49] Deng W, Lai M-J, Peng Z, Yin W. Parallel multi-block ADMM with o(1/ k) convergence. J Sci Comput 2017;71:712–36. https://doi.org/10.1007/s10915-016-0318-2.
[50] Nocedal J, Wright SJ. Numerical Optimization. 2nd ed. New York: Springer; 2006.
[51] West DB. Introduction to graph theory 2001;2.
[52] Hu M, Fukushima M. Variational inequality formulation of a class of multi-leader-follower games. J Optim Theory Appl 2011;151:455–73. https://doi.org/10.1007/s10957-011-9901-8.
[53] Hori A, Tsuyuguchi D, Fukuda EH. A method for multi-leader-multi-follower games by smoothing the followers' response function. 2023.